Journal of Cleaner Production 447 (2024) 141524

Contents lists available at ScienceDirect

Journal of Cleaner Production

journal homepage: www.elsevier.com/locate/jclepro

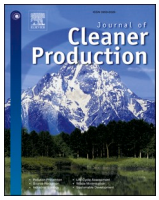

Eco-friendly modification of bitumen: The effects of rubber wastes and castor oil on the microstructure, processability and properties

Maciej Sienkiewicz [a,*], Przemysław Gnatowski [a], Mateusz Malus [b], Anna Grzegórska [c], Hossein Ipakchi [d], Maryam Jouyandeh [e], Justyna Kucińska-Lipka [a], Francisco Javier Navarro [f], Mohammad Reza Saeb [g]

[a] Department of Polymer Technology, Faculty of Chemistry, Gdańsk University of Technology, 80-233, Gdańsk, Poland
[b] Department of Chemistry and Technology of Functional Materials, Faculty of Chemistry, Gdańsk University of Technology, 80-233, Gdańsk, Poland
[c] Department of Process Engineering and Chemical Technology, Faculty of Chemistry, Gdańsk University of Technology, 80-233, Gdańsk, Poland
[d] Department of Chemical Engineering, McMaster University, Hamilton, Canada
[e] Center of Excellence in Electrochemistry, School of Chemistry, University of Tehran, Tehran, 14176-14411, Iran
[f] Pro2TecS-Chemical Process and Product Technology Research Centre, Department of Chemical Engineeing, ETSI, Campus de "El Carmen", University of Huelva, 21071, Huelva, Spain
[g] Department of Pharmaceutical Chemistry, Medical University of Gdańsk, J. Hallera 107, 80-416, Gdańsk, Poland

ARTICLE INFO

Handling editor: Zhen Leng

Keywords:
Bitumen modification
Castor oil
Waste tires recycling
Reclaimed rubber
Rheological properties
Epoxy resin

ABSTRACT

The bitumen industry in the European Union is facing several difficulties, including rising demand, unstable oil supply, rising prices for synthetic polymer modifiers, and a focus on lowering carbon footprint. Bitumen modification with crumb rubber (CR) is one of the most promising solution to these challenges. However, CR-modified bitumen have poor processability and low storage stability. To overcome these flaws we are introducing a sustainable approach for ecological modification of bitumen taking advantage of renewable resources. For this reason, unmodified castor oil was selected as a green modifier of reclaimed rubber dust. The ecologically modified bitumen underwent visco-elastic behavior analysis based on rheological tests varying the temperature. The modification with rubber-oil improved the longevity of typical pavement, featured by an exceptional deformation resistance at elevated temperatures (well above 70 °C, the maximum pavement temperature reported in the region). The Cole-Cole graphs and black space diagrams unraveled the enhanced elasticity of bitumen. Technically, in comparison to plain bitumen, the compatibility ratio of modified bitumen to aggregates showed an uplift by 258%. The environmentally friendly bitumen modified ecologically herein revealed potential for performance window enlargement. Nevertheless, future investigations should focus on optimization of the bitumen formulation, along with examination of other sustainable moieties for the sake of commercialization of the developed binders in pavement construction.

1. Introduction

Many governments are currently dealing with serious environmental problems brought on by improper or inadequate solid waste management, which is exacerbated by the disposal of the end-of-life tires (EOLTs) (Agudelo et al., 2019), as well as an annual increase in the number of vehicles on the road (Eurostat, 2019). Bitumen usage is projected to be 102 million tons annually worldwide, of which 85% is used for stone-based asphalt roads, 10% is used for roofs, and 5% is used for a variety of other purposes, including waterproofing, adhesives, corrosion protection, and automobiles (Jamal and Giustozzi, 2020). The combination of increasing number of vehicles with the advancing climate changes arising from the usage of unsustainable materials results in faster than expected wear of asphalt pavements. The worn asphalt surface, in turn, increases the wear of the car tires while driving. As a result, it was observed that most microplastics were derived from asphalts and car tires (Baensch-Baltruschat et al., 2020; Järlskog et al., 2020; Luo et al., 2021). It is mainly related to the purely physical nature of the interaction of thermoplastic elastomers and waste tire rubber grains with bitumen and the lack of their chemical bonding (Fathollahi

* Corresponding author.
E-mail address: maciej.sienkiewicz@pg.edu.pl (M. Sienkiewicz).

https://doi.org/10.1016/j.jclepro.2024.141524
Received 12 July 2023; Received in revised form 25 January 2024; Accepted 27 February 2024
Available online 28 February 2024

et al., 2022; Rødland et al., 2022) in the pavements. Loosen particles are then released directly into the atmosphere by the wind. It has also been proven that bitumen could be the source of volatile organic compounds (VOC) and particulate matter (PM), which is an underestimated problem, especially in big agglomerations (Borinelli et al., 2020; Van Hal et al., 2019). One of main ways to improve the bitumen quality and service time is the modification of bitumen, preferably by green and sustainable reinforcing agents.

Studies showed there are three main routes for modifications of bitumen: the use of synthetic elastomers (75%) based on styrene (styrene-butadiene-styrene - SBS, styrene-ethylene-butylene-styrene - SEBS), the use of synthetic plastomers (15%) (polyethylene - PE, polypropylene - PP, ethylene vinyl acetate copolymer - EVA) (Tauste--Martínez et al., 2021) or more "green" approach, i.e. the use of waste, mainly rubber (10%) from waste tires (Borinelli et al., 2022; Sol-Sánchez et al., 2020). The low usage of waste materials in asphalt formulations significantly limits the development of this waste recycling technology, but also has a detrimental effect on the environment. The low utilization of waste is mainly caused by the differences in waste components physical properties, such as density or surface tension, and low compatibility of polymer waste with bitumen matrix due weak chemical interactions. The reduction of road industry impact on climate is also executed by usage of reclaimed asphalt (Daryaee et al., 2020; Malinowski et al., 2022). However, this approach is still limited due to performance concerns comming from the presence of aged bitumen, mainly connected with high stiffness and possible fatigue cracking. In the face of climate change, it is obvious that green approaches must be developed and a move towards sustainable raw materials has to be made. Studies in this direction have been conducted in recent years. Hong et al. researched the impact of process variables on the characteristics of waste low-density polyethylene (LDPE) and EVA modified asphalt. According to their findings, LDPE has a greater impact than EVA on asphalt's ability to resist temperature. Furthermore, increased viscosity favors the improvement of the bonding qualities between asphalt and aggregate (Hong et al., 2022). The physical, chemical, thermal and rheological properties of recycling EOLTs in the form of crumb rubber (CR) modified bitumen (CRMB) were investigated by Jamal and Giustozzi. According to the multiple stress creep recovery (MSCR) test, the results showed that tiny additions of CR can greatly increase the rutting resistance of CRMB. Moreover, the addition of CR reduces J_{nr} by 63% while improving R by thirteen times at 3.2 kPa in comparison to regular bitumen (Jamal and Giustozzi, 2020). This approach has some downsides, though. Modification of bitumen with CR results in a significant increase in the viscosity of the rubber-bitumen compositions due to the swelling of rubber grains in result of the absorption of aromatic oils contained in the bitumen, as well as their instability in liquid storage conditions due to the difference in density between rubber and bitumen (Shu and Huang, 2014; Zheng et al., 2021).

The problems related to the use of CR for bitumen modification can be overcome by replacing them with a rubber-oil composition (RO). In this study, RO was obtained in the process of thermo-mechanical devulcanization of rubber dust (RD) in the presence of naturally extracted castor oil (CO). CO was introduced as a plasticizer, facilitating the devulcanization of rubber. In addition, the purpose of CO use was to increase the dispersion of RD in bitumen, which would allow for achieving higher stability of rubber-bitumen binders during storage and transport. However, devulcanization leads to the destruction of the cross-linked structure of rubber, as a result of which it loses the ability to improve the physical and mechanical properties of rubberized binders, leading to an increase in penetration and a greater susceptibility to rutting (Fathollahi et al., 2022). Therefore, in addition to the RO/bitumen composition, an epoxy resin (ER) was used to modify the bitumen, as a compound that chemically bonds all the components of the composition. Conventionally, ER is used in asphalts with curing agents as two- or three-component mixtures (Xie et al., 2022). The structural performance of epoxy asphalt mixture (EAM) is significantly better than that of traditional hot and warm mixture asphalt, according to Jamshidi et al. The binder's high stiffness and strong binding of aggregate particles and binders can be used to enhance EAM's structural performance. Therefore, a variety of marketable waste materials, including CR, waste PE or used cooking oil, are compatible with epoxy asphalt technology (Jamshidi et al., 2022). Commercial copolymer modifiers based on compounds with glycidyl groups are also available on the market (Bulatović et al., 2014; Nizamuddin and Giustozzi, 2022; Pyshyev et al., 2016). In the bitumen modified with SBS and EA, the redistribution of SBS during the SBS-EA securing process was observed. Some of the SBS was seen to interact with ER and greatly improve the compatibility of EA in bitumen matrix. Some of SBS permeated into the epoxy resin phase and served as a bridge of epoxy resin phase and the SBS-asphalt phase (Xu et al., 2022). Based on these findings, the ER utilized in this study is used without employment of curing agents to allow the reactions with the –OH and –COOH functional groups present in CO and simultaneously with the –NH, –SH, –COOH, and –OH groups of bitumen components (Cuadri et al., 2020) and, in turn, increase continuity of CR modified bitumen. As a result, it should constitute a kind of "link" between the reclaimed material and the bitumen, which, in turn, allows it to bind all the components and create a stable, polymeric network, preventing the separation of rubber from the bitumen.

In the light of above discussions and in line with sustainability and green manufacturing strategies worldwide (Wiśniewska et al., 2023a, 2023b), there is a need for using renewable and sustainable ingredients to modify bitumen. The purpose of this study was to establish a new concept into the use of rubber wastes for bitumen modification, taking advantages of plasticization and devulcanization by using natural oils and polymer resins highly reactive with both bitumen and RO material. The main objective of this work was to obtain high-performance bitumen materials reinforced with natural and recycled resources abundantly available on the market without using an external catalyst. Typically, the incorporation of epoxy resin into bitumen for modification of processing behavior and properties needs association of curing agents and/or catalysts (Xie et al., 2022). The present work takes advantage of crosslinking bitumen in the absence of curing agents and catalysts, which lies among few reports available. Another specific feature of this work is the analysis of the stability and effect of thermal ageing of ER-modified bitumen. Although plasticization of rubber with oil is not a new concept, the majority of experimental works utilize the fossil-based oils, like the used engine oil (Li et al., 2023; Liu et al., 2022), waste natural oils, like cooking oil (Xu et al., 2023; Yang and Dong, 2022) or modified natural oils, like oxidized oil residues (Zeng et al., 2016; Zhang et al., 2023). The present study serves the benefit of lowering the environmental burden, definitely being one of the first attempts on the use of natural castor oil without additional treatment in modification of bitumen. The castor oil, which was extracted from *Ricinus communis* seeds, along with rubber dust, was used, which could principally be promising in view of recycling and environmental protection. The effect of the renewable and structural modifiers on the lubricity of the formulated binder was determined for as-mixed and aged samples using rheological experiments applying dynamic shear rheometer (DSR) under different temperatures. Additionally, fluorescence microscopy (FM) was used to investigate how modifiers and bitumen were distributed and contact angle was used to estimate the possible compatibility between obtained binders and mineral aggregates.

2. Materials and methods

2.1. Materials

In the study the following materials were used: 70/100 bitumen (Lotos Asfalt (Lotos, 2023)) (PG 58–22/60S-22 AASTHO M320/M332), Epidian 6 epoxy resin (Ciech (2023)) (epoxide equivalent weight = 185, viscosity at 25°C = 13 Pa s, density at 20°C = 1.15 g/cm^3), DIN Quality/Pale Pressed castor oil (Overlack (2023)) (viscosity at 20°C = 1.05

Pa s, density at 20°C = 0.96 g/cm^3, saponification value = 181 mg KOH/g), rubber dust (GUMEKO) (fraction <0.8 mm).

2.2. RO preparation

In the first stage of the process of preparing a RO, a mixture of RD and CO was prepared using a paddle mixer. The mix consisted of 90 wt% of RD and 10 wt% of CO. Then, the mixture was transferred to a batch mixer (Brabender GMF 106/2), where thermo-mechanical devulcanization/depolymerization of the mixture was carried out. In each case, about 50 g was mixed at 180°C for 30 min, with the rotor speed of 140 rpm. As a result of the above-described process, a plastic RO was obtained.

2.3. Bitumen modification with RO and ER and viscosity test

The bitumen modification process was carried out in steel cans of 1.2 L capacity. The process was split into a few phases. In the first step, a can filled with approximately 700 g of bitumen was heated up in a laboratory dryer at 180°C for 90 min to melt the bitumen. In the next phase, the can was transferred into a homogenization system consisting of a heated plate, thermocouple, and homogenizer (IKA T50 basic ULTRA-TURRAX with M1 [S 50 N – G 45 M] rotor). Bitumen was then mixed (~4000 rpm) and heated up to reach 180°C. Then, the temperature was kept at this point until the end of the modification. After reaching the set temperature, a defined amount of RO was slowly introduced into bitumen and mixed for 15 min. In the next phase, a set amount of ER was introduced into the mixture and homogenized for 45 min, so the summarized modification time was 60 min. After the modification, the viscosity test was performed. The type 3 rotor of the viscometer (Thermo Scientific HAAKE Viscotester 2 Plus) was submerged into bitumen mixture together with the thermocouple. The result was obtained at 160°C. The resulting modified bitumen was then poured into penetration test vessels, softening point rings, high-temperature storage stability tubes, and storage cans for usage in other tests. Ten bitumen samples were prepared: one unmodified, three modified with ER, two modified with RO, and five modified with both ER and RO. Samples were named by the code: ERxROxx, where x was the wt.% of the component in bitumen composition. Used ER content was 0, 4, 5 and 6 wt%, whereas RO content was 0, 15 and 20 wt%.

2.4. Penetration and softening point tests

The penetration test was performed according to PN-EN 1426 standard using a penetrometer (Petrotest PNR 12). According to the standard, the result was mean from at least three results differing maximally by 1 [0.1 mm] from each other. The Softening point test was performed as a ring and ball test according to PN-EN 1427 standard using a test kit (Petrotest, Softening-Point - Ring & Ball Method [manual]). The softening point was the mean from the temperatures of each ring and ball tests, which were not differing by more than 1°C from each other.

2.5. Bitumen stability testing during storage

To determine the bitumen storage stability, a tube test according to the PN-EN 13399 standard was conducted. The result of the test was the difference between the penetration value and the softening point between the upper and lower parts of the sample. According to the PN-EN 14023 standard, bitumen was considered stable when the difference in softening point was not greater than 5°C.

2.6. Rheology

For rheology studies, a dynamic shear rheometer with controlled shear stress (Anton Paar Physica MCR 301) was used. Using this device, three tests were conducted: dynamic viscous flow, temperature sweep test, and MSCR. All tests start with heating up a bitumen sample to 60°C on a heated plate, pressing it to the test gap height with the rotor, and trimming the excess bitumen sample, which flowed outside of the rotor before testing. The sample was then thermostated at the test starting temperature for 20 min.

The temperature sweep test was used to determine the storage modulus G′ [Pa], the loss modulus G″ [Pa], and tan δ. $|G^*| = (G'^2 + G''^2)^{1/2}$ [Pa] represents the absolute value of the shear complex modulus. The oscillating temperature sweep test allows to study the temperature characteristics of the sample, glass transition temperature, softening or melting, as well as the study of the crystallization and sol-gel transformation process. In this test, the rotor oscillates with set frequency to deform the sample by set value. For each measuring point, the information about G′ and G″ was gathered for 20 s. Sample was then heated up to the next measuring point and thermostated for 1 min. Based on temperature sweep test results, Upper Critical Temperature (UCT) can be estimated from $|G^*|/\sin\delta$ parameter (also known as rutting parameter), which was introduced by USA Strategic Highway Research Program (SHRP) in 1987 to assess whether the binder meets the requirements for rutting resistance. According to AASHTO M 320, UCT can be established when $|G^*|/\sin\delta$ parameter reaches 1 kPa or 2.2 kPa for unaged and aged bitumens, respectively. After exceeding UCT during pavement usage, the rutting effect of the pavement made of this type of bitumen could be expected.

Dynamic viscous flow measurements were carried out at two temperatures: 60 and 135°C in a relatively wide range of shear rates (10^{-4} – 10^4 s^{-1}). Apparent viscosity data were collected every 2 min upon reaching steady state.

The MSCR test was used to determine non-recoverable creep compliance (J_{nr} [kPa^{-1}]) and percent recovery (R [%]) to determine the binder's influence on the resistance of the bitumen mixture to permanent deformation-rutting, as well as the assessment of the effectiveness of asphalt modification. MSCR test was performed at 60°C according to EN 16659 standard. The scheme of obtained parameters was presented in Fig. 1. R and J_{nr} for each cycle were calculated using following formulas:

$$J_{nr} = \frac{\varepsilon_r}{s} \left[kPa^{-1}\right] \quad (1)$$

$$R = \frac{100\% * (\varepsilon_c - \varepsilon_r)}{\varepsilon_c} [\%] \quad (2)$$

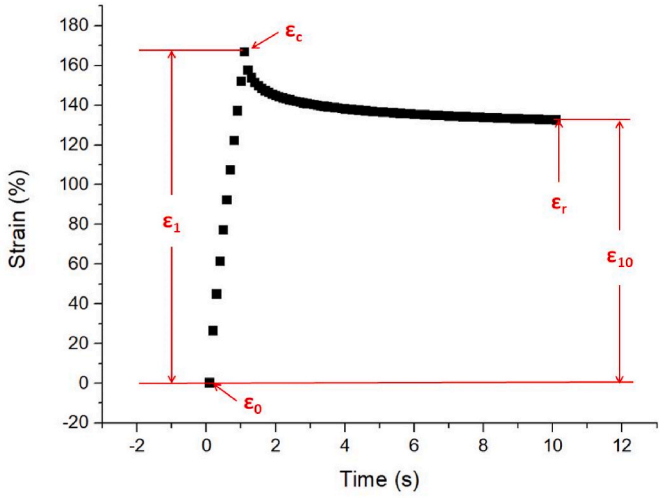

Fig. 1. Diagram showing the example time dependence of deformation for the MSCR test. ε_0, ε_1, ε_{10} are the strain of bitumen sample at the beginning of cycle, after 1 s of stress and at the end of the cycle. ε_c is the maximal strain observed during the cycle and ε_r is the irreversible deformation.

where: ε_c – maximal strain; ε_r – irreversible deformation; s – applied shear stress.

2.7. Fourier transform infrared spectroscopy

Prior to spectroscopy, samples were prepared as solutions with a concentration of about 0.1 g/mL in tetrahydrofuran. The samples were mixed thoroughly until completely dissolved. Using a Pasteur pipette, drops of the solution were applied to the thoroughly cleaned surface of the measuring cuvette and the solvent was allowed to evaporate. Then the cuvette was placed in the Tensor 27 spectrophotometer (Bruker) with an ATR accessory and the measurement in the wavenumber range 400–4000 cm^{-1} (256 scans) was performed. For spectra analysis, OPUS software (Bruker) was used.

2.8. Optical fluorescence microscopy

An optical microscope equipped with epifluorescence kit (Delta Optical, model: L-1000) and a digital camera (ToupTek Photonics, model: SCCCD01400KPA) were used in this study. A microscope was used in transmission mode for obtaining standard micrographs and in fluorescence mode a mercury lamp was used together with "V" bandpass filter employed (band pass: 400–410 nm, dichroic mirror: 455 nm, band absorption: 460 nm). The ToupView software was used to control the camera. Image post-processing was performed with Fiji ImageJ2 software (Schindelin et al., 2012).

2.9. Contact angle, surface energy, bond energy, and compatibility ratio

For contact angle measurement Rame-Hart 90-U3-PRO equipment and the Drop Image Pro computer program were used. As measurement liquids distilled water, ethylene glycol (EG) (Sigma-Aldrich), and diiodomethane (DJM) (Sigma-Aldrich) were used. Liquids were placed on the surface of the sample using Gilmont GS-1200 Micrometer Syringe in the form of free-dripped droplets formed at 1 cm distance from the sample surface. The contact angle was then measured by the Drop Image Pro program. 10 measurements were taken for each sample and each liquid. Collected data was then used for the calculation of surface energy of solids using the Good–van Oss–Chaudhury model.

The absolute values of aggregate-bitumen bond energies and compatibility ratios (CoR) were calculated according to the method presented by Hefer et al. (2006) (Equations (3)–(8)). Five types of aggregates were considered in calculations: gravel, granite, basalt (data from (Bhasin et al., 2007):), limestone and sandstone (data from (Bhasin et al., 2006):).

$$\Delta G_{ab}^{abs\ dry} = 2\sqrt{\gamma_a^{LW}\gamma_b^{LW}} + 2\sqrt{\gamma_a^{+}\gamma_b^{-}} + 2\sqrt{\gamma_a^{-}\gamma_b^{+}} \tag{3}$$

$$\Delta G_{abw}^{abs\ wet} = \gamma_{aw} + \gamma_{bw} - \gamma_{ab} \tag{4}$$

$$\gamma_{ij} = \gamma_{ij}^{LW} + \gamma_{ij}^{AB} \tag{5}$$

$$\gamma_{ij}^{LW} = \left(\sqrt{\gamma_i^{LW}} - \sqrt{\gamma_j^{LW}}\right)^2 \tag{6}$$

$$\gamma_{ij}^{AB} = 2\left(\sqrt{\gamma_i^{+}} - \sqrt{\gamma_j^{+}}\right)\left(\sqrt{\gamma_i^{-}} - \sqrt{\gamma_j^{-}}\right) \tag{7}$$

$$CoR = \frac{\Delta G_{ab}^{abs\ dry}}{\Delta G_{abw}^{abs\ wet}} \tag{8}$$

where: $\Delta G_{ab}^{abs\ dry}$ – absolute value of work of adhesion between the bitumen and aggregate at their interface in a dry condition, γ^{LW}, γ^{AB}, γ^{+}, γ^{-} – Lifshitz-van der Waals (dispersive), acid-base, acid (electron acceptor), and base (electron donor) components of energy of solid, respectively, a – aggregate, b – bitumen, $\Delta G_{abw}^{abs\ wet}$ – absolute value of free energy released when water displaces bitumen at the bitumen-aggregate interface, w – water, i,j – any of two phases, CoR – compatibility ratio.

2.10. Statistical analysis

Analysis of variance (ANOVA) at $p \leq 0.05$ and post-hoc Tukey test ($\alpha = 0.05$) were used to evaluate the significance of the ER and RO addition into the bitumen matrix.

3. Results and discussion

3.1. Dynamic viscosity, penetration, and softening point

The values of viscosity of bitumen after modification, penetration and softening point before and after the tube test were presented in Table 1.

In comparison to neat bitumen (ER0RO0), the viscosity of ER-modified samples (ER4-6RO0) at 160°C has slightly increased (by 0.01–0.02 Pa s). In comparison to neat bitumen, the viscosity of RO-modified (ER0RO15-20) samples has dramatically increased (by 0.15 and 0.20 Pa s, respectively), which was also significant according to ANOVA. For RO15 samples, adding ER to RO-modified bitumen resulted in a minor drop in viscosity (by maximum 0.05 Pa s), however, for RO20 samples, an increase in viscosity after adding ER was noted (by 0.09 Pa s).

The softening point of ER-modified samples (ER4-6RO0) have slightly increased (by ~2°C) in comparison to neat bitumen (ER0RO0). The softening point of RO-modified (ER0RO15-20) samples has significantly increased (by 4.1 and 5.4°C respectively) in comparison to neat bitumen, which was also significant in ANOVA. The addition of ER into RO-modified bitumen did not change softening point in the case of RO15 samples, but for RO20 increase in softening point after the addition of ER was observed (by ~1°C).

The penetration of ER-modified samples (ER4-6RO0) did not significantly differ from neat bitumen (ER0RO0) values. In the case of RO-modified samples (ER0RO15-20) plasticization of bitumen could be observed (penetration increased by ~20 [0.1 mm]). The addition of ER into RO-modified bitumen (ER4-6RO15-20) resulted in a slight decrease of penetration (by ~5 [0.1 mm]) compared to neat bitumen.

Concerning results after the stability test, according to PN-EN 14023 standard, all prepared samples were considered stable (Δ penetration <9 [0.1 mm]; Δ softening point <5°C). The highest deviation in both penetration and softening point was observed for the ER4RO15 sample, but it was still considered stable.

In the case of ER-modified samples (ER4-6RO0) a significant decrease in penetration and increase of softening point after stability test was observed compared to samples after homogenization, confirmed with ANOVA. This suggests that the additional heating time allowed the reaction of epoxy groups to take place and to form a polymeric network in the asphalt binders. The more ER was present in the composition, the lower was penetration and the higher softening point. It was true for all ER-containing samples.

Penetration of RO-modified bitumen (ER0RO15-20) after the stability test was significantly higher than the value determined after homogenization of the binders, which indicates that the bitumen was plasticized under the influence of de-vulcanized rubber and castor oil, or further rubber digestion (devulcanization/depolymerization) took place under storage conditions. The softening point change after the stability test was insignificant, as it was lower (~1°C) than the samples after homogenization.

In case of ER5RO20 sample the evidence of partial cross-linking reaction during the homogenization could be spotted: significant increase in viscosity (by 0.095 Pa), slight increase in softening point (~1°C) and decrease in penetration (6 [0.1 mm]) comparing to ER0RO20. Samples

Table 1
Bitumen composition, the values of bitumen viscosity after modification, penetration, softening point after homogenization and storage stability test.

Sample name	Composition wt.%		Results								
			After homogenization			After stability test					
	ER	RO	Viscosity [Pa.s/ 160 °C]	Penetration [0.1 mm]	Softening point [°C]	Penetration [0.1 mm]			Softening point [°C]		
						Top	Down	Δ penetration	Top	Down	Δ softening point
ER0RO0	0	0	0.04	74	45.7	80	81	1	46.8	46.9	0.1
ER4RO0	4	0	0.06	70	47.8	35	34	1	62.5	62.2	0.3
ER5RO0	5	0	0.05	75	47.2	33	32	1	64.7	64.8	0.1
ER6RO0	6	0	0.06	73	47.3	29	29	0	67.5	67.3	0.2
ER0RO15	0	15	0.19	93	49.6	102	98	4	47.3	50.6	3.3
ER4RO15	4	15	0.17	87	50.4	59	54	5	55.1	60.0	4.9
ER5RO15	5	15	0.14	90	50.2	53	52	1	60.0	60.4	0.4
ER6RO15	6	15	0.18	91	50.0	46	47	1	65.0	63.7	1.3
ER0RO20	0	20	0.24	94	51.3	114	108	6	47.5	49.7	2.2
ER5RO20	5	20	0.33	88	52.2	59	63	4	62.1	64.1	2.0

of ER and RO-modified bitumen (ER4-6RO15-20) after the stability test demonstrated a significant decrease in penetration and an increase of softening point in comparison to to samples after homogenization. The behavior was similar to ER-modified samples (ER4-6RO0), which suggests that cross-linking reaction was taking place with bitumen components besides RO presence. However, ANOVA suggest that interaction between ER and RO is significant at 95% confidence level. This explanation is further supported by lack of an important ageing and properties change of neat bitumen under storage conditions.

Literature reports increasing viscosity with the addition of both ER and crumb rubber (Çubuk et al., 2009; Wang et al., 2012). The literature does not report results after the tube test for the ER-modified bitumen. In the case of properties after homogenization, it is reported that usage of ER as bitumen modifier results in a slight increase of softening point and a decrease in penetration - 3°C and 8 [0.1 mm], respectively for standard 50/70 bitumen grade (Çubuk et al., 2009) and 11°C for oxidized 50/70 bitumen grade (Motamedi et al., 2017) modified with 2 wt% of bisphenol A based ER. In the case of oxidized bitumen, a slight increase in Shore A hardness was observed, which corresponds to observed penetration decrease observed in our research. For comparison, bitumens modified with epoxidized soybean oil, a similar behavior to our ER-modified bitumens was observed: increase of softening point by 2°C and penetration decrease by 2 [0.1 mm] after the addition of soybean oil (Yin et al., 2013). In the case of bitumen modified with RO, a similar increase of penetration was observed for bitumen modified with waste cooking oil and tire rubber (Khan et al., 2019), but also decrease in softening point was observed here. Also, similar results were obtained with waste engine oil and crumb rubber for bitumen 60/90 grade

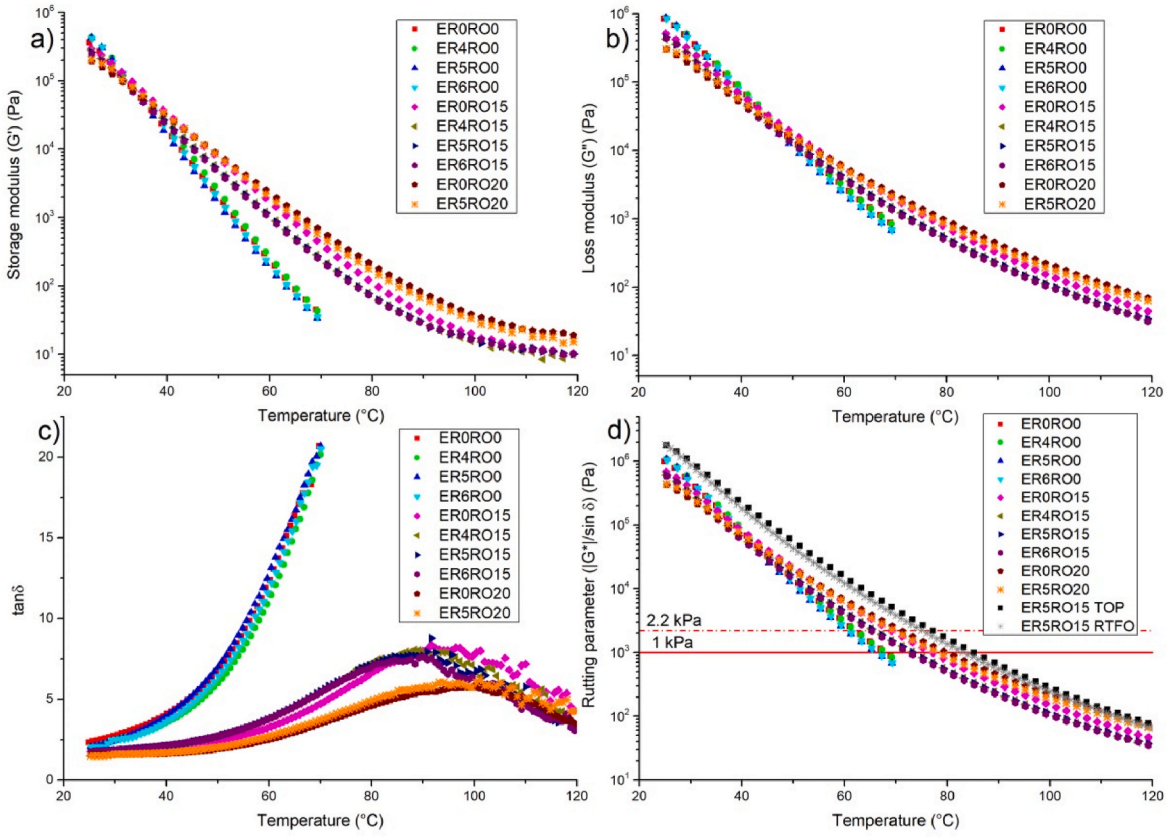

Fig. 2. Temperature dependence of a) storage modulus, b) loss modulus, c) tan δ and d) |G*|/sin δ rutting parameter in temperature sweep test of bitumen samples.

(Tileuberdi et al., 2013) and with bio-oil crumb rubber for bitumen 70# grade (Xue et al., 2023): penetration was increasing with RO content together with softening point. In most publications, it is reported that usage of CR increases softening point and decreases penetration (Khan et al., 2019; Tileuberdi et al., 2013; Yao et al., 2018). It is also known that the storage stability of CR modified bitumen samples decreases with particle size and storage temperature.

3.2. Rheology

The results of temperature sweep tests were displayed in Fig. 2. For all samples, the values of the storage modulus and the loss modulus (Fig. 2a and b) decreased with increasing temperature. Results for samples without rubber (ER0-6RO0) were analyzed up to 70°C due to the instrument limitations in control deformation mode and low sensitivity at the selected deformation of these low-viscous materials.

In the case of ER-modified samples (ER4-6RO0) very similar values of G′, G″, and tan δ in comparison to neat bitumen were observed, thus their performance in uncured state will be similar to neat bitumen. Concerning RO-modified bitumen (ER0RO15-20) samples, with increasing amounts of RO, both G′ and G″ values were decreased in lower temperatures and increased in higher temperatures in comparison to neat bitumen. Lower thermal susceptibility of RO-modified bitumen samples was also observed (lower slopes of G′ and G″ with temperature, in comparison to neat bitumen). At high in-service temperatures, the higher value of the storage modulus results in higher resistance to permanent deformation or rutting. On the other hand, if this value was too high, at intermediate and low temperatures, bitumen could become brittle and cracking at low temperatures could occur. Accordingly, it was most preferred that the modified bitumen exhibits a higher G′ value at high temperatures and lower at low temperatures. The results clearly indicate that increasing the amount of RO improves resistance to permanent deformation and rutting at high temperatures, and also suggest a reduction in brittleness at lower temperatures. Addition of ER into RO-modified bitumen (ER4-6RO15-20) results in slight decrease in both G′ and G″, which suggests the plasticizing effect of the ER in RO-modified bitumen during homogenization. The decrease did not differ between samples with different ER amounts (ER4-6RO15).

In Fig. 2c the tan δ relation to temperature was shown. The neat bitumen exhibits a predominately viscous behavior (tan $\delta > 1$) across the whole tested temperature range, which was particularly apparent at higher temperatures. Similar behavior was seen in all samples of bitumen that had undergone ER modification (ER4-6RO0). The curves "flattened" and the tan δ value fell in the case of modification with RO or ER and RO (ERxRO15-20), indicating that these systems were more resistant to temperature changes and had improved elastic behavior.

It is noteworthy the appearance of a loss tangent peak at high temperatures, which has been frequently related to the collapse of colloidal bitumen microstructure of asphaltene micelles surrounded by solid resin. As this transition shifts to higher temperatures, bitumen stiffness increases and, therefore, the performance at high temperatures is enhanced (Romera et al., 2006). In general, it is clear that RO concentration is the major parameter affecting this peak temperature.

The analysis of rutting parameters (|G*|/sin δ) (Fig. 2d–Table 2) for bitumen samples shows an increase of UCT from 67.9°C (for neat bitumen) to 79.6°C for (for ER0RO20). Similarly, to storage and loss modulus, ER alone does not affect the behavior of bitumen, but the RO addition significantly increases the UCT parameter value, which is confirmed by ANOVA. ER in RO-modified bitumen slightly lowers the rutting parameter. Once again, it seems that the addition of ER to bitumen after homogenization yields a slight softening due to the low viscosity of the added reagents and further hardens during tube test and RTFO tests as a consequence of the progress of the chemical reactions with time. In the case of sample ER5RO15, UCTs (G*/sin $\delta > 2.2$ kPa) after stability (77.0°C) and RTFO test (75.5°C) were significantly higher than corresponding unaged sample.

Table 2
Estimation of Upper Critical Temperature (UCT) based on |G*|/sin δ rutting parameter.

Sample Name	UCT (°C)
ER0RO0	67.9
ER4RO0	67.5
ER5RO0	65.7
ER6RO0	65.7
ER0RO15	75.9
ER4RO15	71.9
ER5RO15	71.6
ER6RO15	71.7
ER0RO20	79.6
ER5RO20	77.8
ER5RO15 TOP	77.0
ER5RO15 RTFO	75.5

The findings of rutting parameter correspond to the literature, where, in general, addition of crumb rubber increases this parameter (Jeong et al., 2010; Yao et al., 2018). In the case of crumb rubber-modified bitumen created with the use of waste frying oil (Bilema et al., 2021) and bio-oil (Xue et al., 2023), an increase in rutting parameter was also observed. Rheological findings for ER modification also correspond to the literature, where no significant effect of non-cured ER on both G′ and G″ is observed (Cuadri et al., 2020).

Fig. 3 reveals the temperature dependence of storage and loss modulus of (ER5RO15) sample after homogenization, storage stability and RTFO tests. The values of both modules for the top and bottom parts of the bitumen sample do not differ, which confirms that the bitumen modified with 5 wt% of ER and 15 wt% of RO was stable after tube test. After additional thermal ageing, a significant increase in the value of both the storage modulus (G′) and the loss modulus (G″) could be also noticed. This behavior, together with softening point and penetration changes, allows concluding that a longer heating time was needed to induce a chemical reaction between the epoxy groups of the resin and the reactive groups present in the bitumen group components, which affects the formation of a polymer network in the bitumen and improvement of the rheological properties of the rubber-bitumen binders obtained in this way.

A Cole-Cole (C–C) plot can be used to visually display the viscous and elastic parts of the material's stiffness. It demonstrates how elastic components (storage modulus) and viscous (loss modulus) contribute to the overall stiffness of materials (Dong et al., 2016; Hajikarimi et al.,

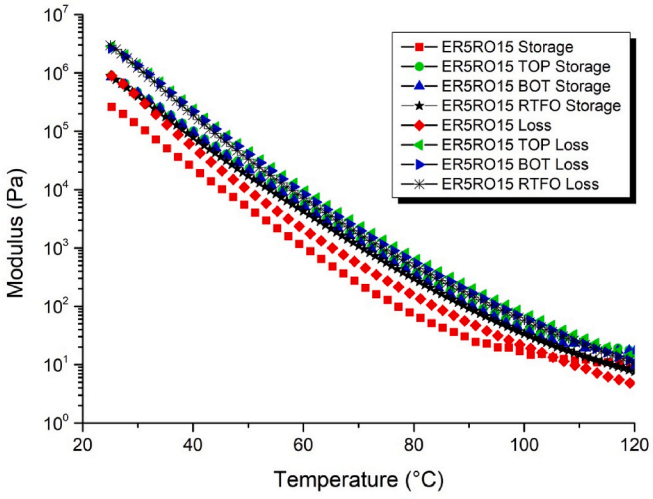

Fig. 3. Comparison of storage and loss modulus in temperature sweep test of ER5RO15 sample after homogenization, tube test and RTFO test. The values of modulus between top and bottom part of the sample after stability are overlapping.

2019). Usually, a C–C plot is drawn between the storage and loss modulus. Fig. 4a depicts the C–C plot for the modified specimens with ER (ERxRO0). As can be shown, neat bitumen is largely unaffected by ER. When RO (Fig. 4b) was added to bitumen, the binders (ER0RO15 and ER0RO20) became more elastic, which is characterized by significantly lowered loss modulus, coupled with appearance of less viscous region. RO addition also resulted in an increase of the total stiffness, which is especially needed in higher temperatures. In comparison, neat bitumen is characterized by a greater loss modulus (G″) value, which indicates that a considerable portion of energy used for deformation is dispersed. The bituminous component's higher viscosity provides adequate flow resistance, while the RO particles' ability to store applied energy and resist deformation improves the material's overall elastic response (Jamal and Giustozzi, 2020). Similarly to the ER only modification, the ER did not influence the RO modified bitumen behavior (Fig. 4c). The heat-treated samples (Fig. 4d) showed small increase in stiffness and decrease of elasticity in low elastic region (ER5RO15 TOP and BOT), whereas the aged sample (ER5RO15 RTFO) showed higher increase in stiffness, retaining elasticity of non-treated sample (ER5RO15).

By graphically representing the relationship between the magnitude of a complex shear modulus (G*) and its corresponding phase angle across different temperature settings, one can construct black space diagrams (BSD). These diagrams serve as a valuable tool in distinguishing between thermo-rheological materials that exhibit simplicity or complexity in their behavior (Kaya et al., 2019). According to Fig. 5, the most viscous behavior is displayed by neat bitumen, which causes it to have the greatest phase angle values. A fully viscous substance has a phase angle of 90°; bitumen's gel-like structure causes the phase angle values to gravitate toward 90° at high temperatures (Kaya et al., 2019; Tan and Guo, 2013). Fig. 5 demonstrates that the phase angle tends toward lower values at low test temperatures. Addition of ER to the bitumen matrix resulted in slight decrease of the stiffness, further supporting the previous findings about plasticizing effect of the ER on bitumen. The BSD is shifted to the left by adding RO, resulting in a smaller phase angle than neat bitumen where the same complex modulus is discovered. With the increase of RO content, more elastic behavior is observed, as evidenced by a decrease in phase angle for a specific complex shear modulus. At elevated temperatures, the higher stiffness and lower phase angle prevents the formation of ruts, thus observed behavior is promising in further applications as asphalt binder. There is a reasonable amount of superposition in the geometry of the black space diagram for both neat and modified bitumen, and the fact, that the phase angle increases gradually as the complex modulus decreases as seen in Fig. 5, further supports the idea that ER-RO modified bitumen does not exhibit phase separation. The ER-RO bitumen must comply with the time-temperature superposition idea in order to establish rheological parameters. Similar outcomes were reported by Zhu in a predictive model for bitumen shear (Zhu et al., 2022).

Figs. 6 and 7 show dynamic flow viscosity of bitumen. For the (ER5RO15) sample after tube test, results of top and bottom parts were comparable and were plotted together as *STAB*. All samples without rubber (ER0-6RO0) showed Newtonian behavior in the whole experimental interval, whereas bitumens with RO are characterized by a Newtonian region at low shear rates, followed by shear-thinning region above a critical shear rate value. In the case of all samples, the influence of ER on bitumen viscosity was inconsiderable at both 60 (Figs. 6a) and 135°C (Fig. 6b). In addition, due to instrument limitations, measurements at 135°C for ER0-6RO0 samples were possible only for shear rates higher than 0.1 s^{-1}. For RO-modified samples (ER0RO15-20), a change in the viscous flow behavior is noticed (from Newtonian to shear thinning) together with a notable increase in viscosity, at both 60 and 135°C,

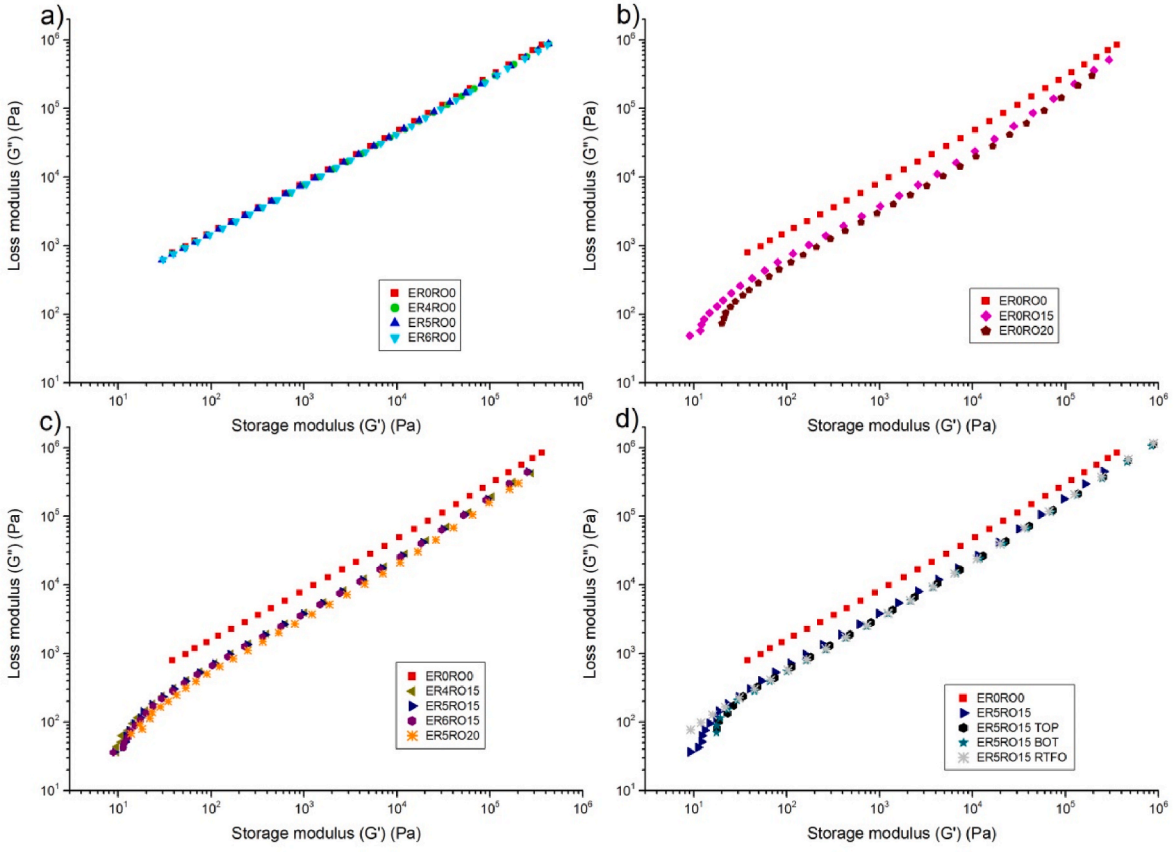

Fig. 4. Cole-Cole plot of a) ER, b) RO, c) ER-RO and d) ER5RO15 modified bitumen. The number of data points was limited to 30 for each curve.

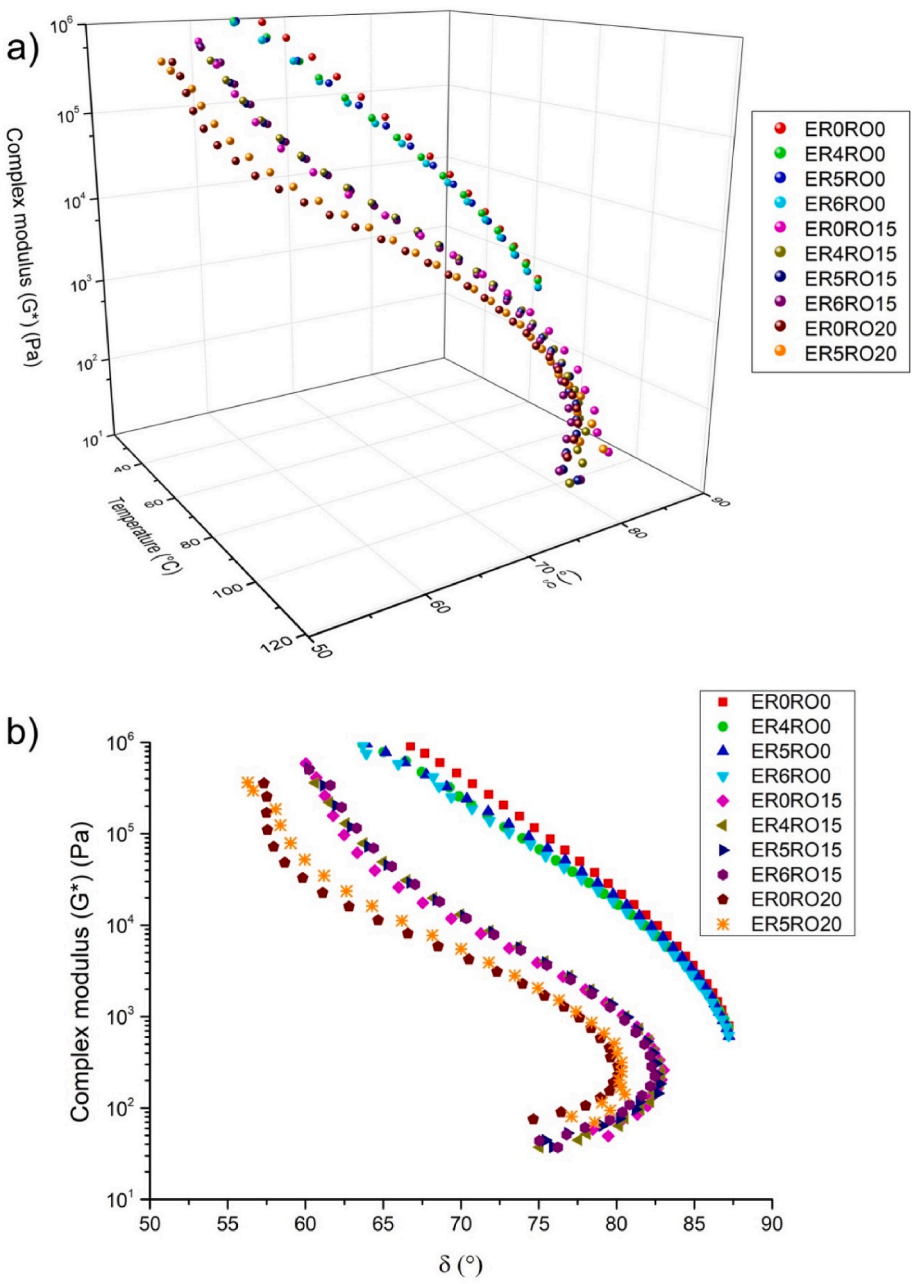

Fig. 5. Black space diagram (BSD) for modified bitumen: a) three-dimensional graph, b) projection on ZY plane (G* and δ). The number of data points was limited to 30 for each curve.

due to the presence of rubber particles. Higher viscosity values were observed for samples modified with 20 wt% of RO. Thus, RO modification, on the one hand, leads to a stronger increase in viscosity, and on the other hand, shifts the critical shear rate for the onset of the shear-thinning region to lower values, which is considered a typical response of more structured binders. At 135°C, the Newtonian region is no longer detected, whereas samples reach a shear-thinning at high shear rates. At this temperature, as bitumen phase is softened and rubber particles still remain solid, the shear thinning character is accentuated. SHRP suggests that viscosity of bitumen at 135°C should not exceed 3 Pa s (Fig. 6b). Obtained samples meet the specification requirement above 0.1 s^{-1} shear rates for samples modified with 15 wt% of RO and above 5 s^{-1} shear rate for samples modified with 20 wt% of RO. Consequently, the SHRP criterion is fulfilled at higher shear rates, well inside the interval where bitumen is pumped, handled and mixed with mineral aggregates. Comparing samples ER5RO15 after homogenization, tube test and RTFO test (Fig. 7) high increase in viscosity could be observed for samples affected by aging. Once again, it could be deduced that a reaction between epoxy resin and other bitumen components has happened. In consequence, cross-linking of bitumen composition resulted in a viscosity increase.

Observed viscous flow behaviors correspond to literature reports, where slight increase of viscosity in both 60 and 135°C in dynamic flow viscosity test for ER-modified bitumen samples (Cuadri et al., 2020) can be observed. Also, a significant increase in viscosity at 135°C was observed for crumb rubber-modified bitumen (Duan et al., 2021; Jeong et al., 2010).

In Fig. 8 results of the bitumen MSCR test were presented. In Table 3 calculations of non-recoverable creep compliance (J_{nr}) and recovery value (R) were presented. Neat bitumen sample and ER-modified samples (ER0-6RO0) showed the typical viscous Newton-type response – a typical staggered layout. They were characterized by large deformation

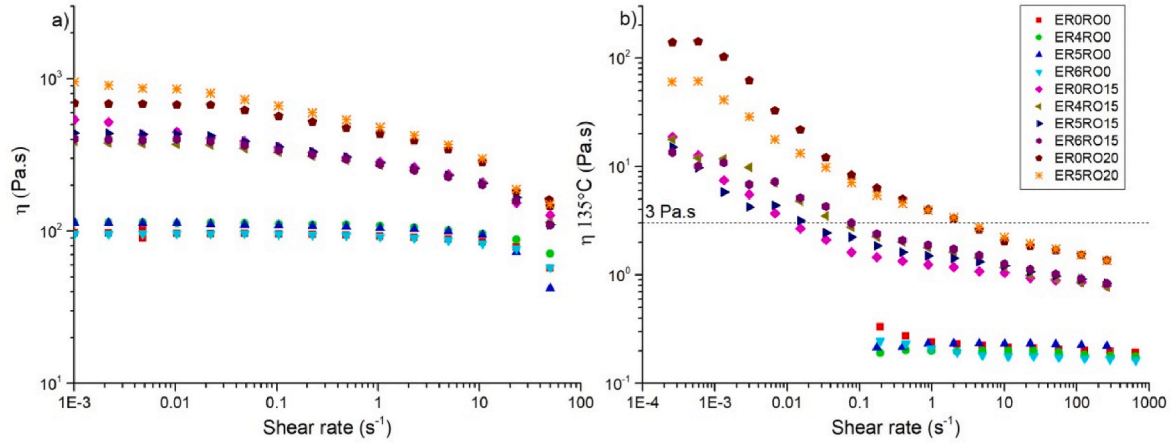

Fig. 6. Shear rate dependence of viscosity in a) 60 °C and b) 135 °C in dynamic flow viscosity test for bitumen samples.

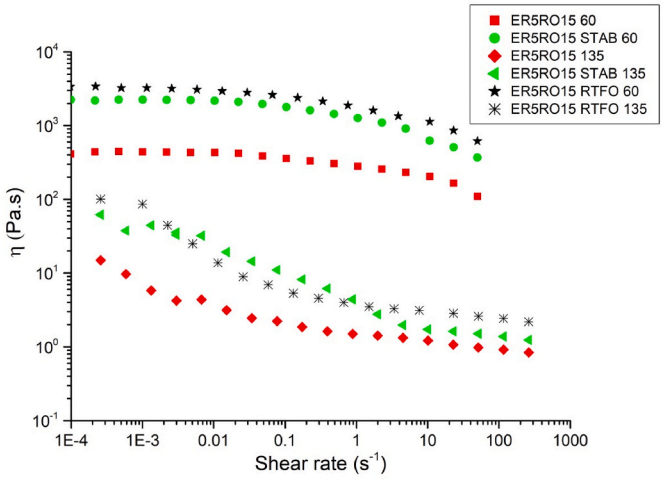

Fig. 7. Shear rate dependence of viscosity in 60 and 135 °C in dynamic flow viscosity test for ER5RO15 bitumen sample after homogenization, tube test and RTFO test.

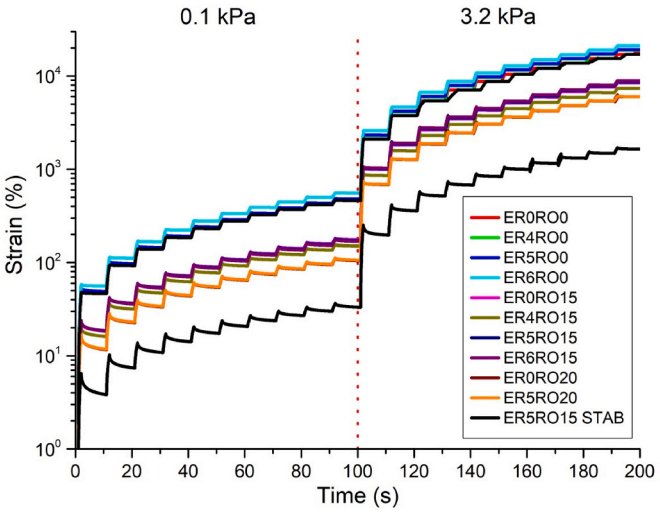

Fig. 8. Time dependence of strain in MSCR test for bitumen samples.

and a lack of elastic recovery of the system after removing the stress. This means that pavements prepared with such bitumen would be susceptible to deformation and fatigue cracking. In case of RO-modified samples (ER0RO15-20) significant decrease of strain is observed with increasing content of RO. In addition, the use of rubber allowed for the improvement of the elastic return (serrated profile), which is greater with the higher RO content in the bitumen. This would allow it to counteract permanent deformation of the pavement during repeated loading. However, this only occurred at a load of 0.1 kPa, while in the case of 3.2 kPa, a staggered pattern is observed with no apparent elastic recovery.

The addition of ER to RO-modified samples (ER4-6RO15-20) did not differ significantly from the properties of the bitumen modified only with the rubber-oil composition. It can be seen that thermal ageing of an (ER5RO15) system helped to improve its resistance to permanent deformation. For this sample (ER5RO15 STAB), a significant reduction in deformation during loading is observed, but also the achievement of siginificant elastic recovery in the case of a load of 3.2 kPa, which was not seen in other samples.

Based on non-recoverable creep compliance (J_{nr}) and recovery value (R) calculations (Table 3), it could be said that the neat and ER-modified bitumen samples (ER4-6RO0) were characterized by a slight elastic recovery of about 3–4% in the case of a load of 0.1 kPa and no elastic recovery (bellow 1%) when the load was 3.2 kPa. These samples were also characterized by a relatively high value of the J_{nr} parameter (higher than 0.5 kPa^{-1}), which showed their high susceptibility to non-recoverable creep, thus low resistance to rutting. The introduction of 15 wt% of the rubber-oil composition to the system caused a significant increase in elastic recovery to about 24% and in the case of 20 wt% RO up to about 37%. For samples ER0RO15-20, a decrease in the value of the J_{nr} parameter was also observed with an increase in the content of RO.

The addition of ER to RO-modified bitumen did not change R and J_{nr}. The statistical analysis also confirmed that only RO had significant effect on MSCR results. However, thermal treatment of the epoxy-modified bitumen sample (ER5RO15 STAB) caused a significant increase in the value of elastic recovery both at the load of 0.1 kPa and 3.2 kPa, to the value of 48% and 27% for STAB. This sample (ER5RO15 STAB) was also characterized by the lowest value of the J_{nr} parameter for both 0.1 and 3.2 kPa. This should result in a significant improvement in resistance to permanent deformation or rutting.

The results of MSCR test are corresponding to the literature, where the addition of rubber significantly lowers J_{nr} and increases recovery of bitumen (Liu et al., 2023; Zhang et al., 2016). Also, a high increase in recovery was observed in ER modified bitumen emulsions after curing (Li et al., 2021), which corresponds to results observed for ER5RO15 samples after tube test and RTFO tests.

Table 3
Non-recoverable creep compliance (J_{nr}) and recovery value (R) based on MSCR test results of bitumen samples.

Sample	R [%]		J_{nr} [kPa^{-1}]	
	0.1 kPa	3.2 kPa	0.1 kPa	3.2 kPa
ER0RO0	3.06 ± 0.71	0.365 ± 0.018	0.4643 ± 0.0036	0.5205 ± 0.0056
ER4RO0	3.62 ± 0.19	0.345 ± 0.013	0.5267 ± 0.0010	0.5992 ± 0.0023
ER5RO0	3.90 ± 0.19	0.379 ± 0.014	0.5140 ± 0.0011	0.5862 ± 0.0029
ER6RO0	4.11 ± 0.43	0.391 ± 0.016	0.5563 ± 0.0022	0.6426 ± 0.0054
ER0RO15	24.3 ± 2.2	4.989 ± 0.039	0.1759 ± 0.0049	0.2585 ± 0.0015
ER4RO15	25.8 ± 3.3	5.36 ± 0.32	0.1504 ± 0.0054	0.2255 ± 0.0099
ER5RO15	26.7 ± 3.6	4.73 ± 0.88	0.172 ± 0.016	0.264 ± 0.015
ER5RO15 STAB	48.2 ± 3.8	26.5 ± 1.8	0.0331 ± 0.0035	0.0502 ± 0.0037
ER6RO15	29.0 ± 2.9	4.73 ± 0.61	0.1686 ± 0.0097	0.2723 ± 0.0076
ER0RO20	37.6 ± 3.5	8.85 ± 0.33	0.1043 ± 0.0092	0.1843 ± 0.0067
ER5RO20	36.2 ± 2.9	7.67 ± 0.12	0.106 ± 0.059	0.1850 ± 0.0066

3.3. Fourier transform infrared spectroscopy

For the analysis of the degree of cross-linking of the epoxy resin, spectra in the wavenumber range of 1300–850 and 1800-1550 cm^{-1} were used (Fig. 9). Analysis has focused on the disappearance of the bands originating from the epoxy groups, at a wavelength of around 915 cm^{-1}, which are specific for the valence vibrations of the epoxy group in the non-cross-linked resin.

In the case of a bitumen sample modified with 5 wt% of ER (ER5RO0), the presence of a band of epoxy groups (912 cm^{-1}) was observed. For the ER4RO15 sample, which had the addition of 15 wt% of RO, this band was not observed. Its disappearance is one proof of the reaction of the epoxy groups of the resin with castor oil incorporated into rubber, most probably due to the ester exchange reactions in consequence of the first stage of cross-linking in this bitumen system. In ER and all bitumen samples the C–O–C stretching band of ether linkage around 1035 cm^{-1} was found. In all epoxy-modified bitumen samples, the disappearance of 1070 cm^{-1} C–O band from terminal rings was observed. In a region of 1740 cm^{-1} stretching bands of C═O linkage can be spotted for castor oil and bitumen samples modified with RO. Comparing the ER4RO15 bitumen sample after homogenization and stability test no significant differences are observed. However, for the RTFO sample, the appearance of a band at 1245 cm^{-1} with the disappearance of 1262 cm^{-1} band can be observed, similar to the ER5RO0 sample. The band of 1245 cm^{-1} can be associated with the C–O stretching bond of forming ester groups, while 1262 cm^{-1} band can be attributed to C–O bonds of aryl rings found in asphaltenes phase (Koyun et al., 2021). Similar observations on structure of ER and RO modified bitumens can be found in literature (Bilema et al., 2021; Poulikakos et al., 2014). Therefore, FTIR observations are in line with the rheological results and confirm the enhanced progress of epoxy groups chemical reactions during RTFO ageing.

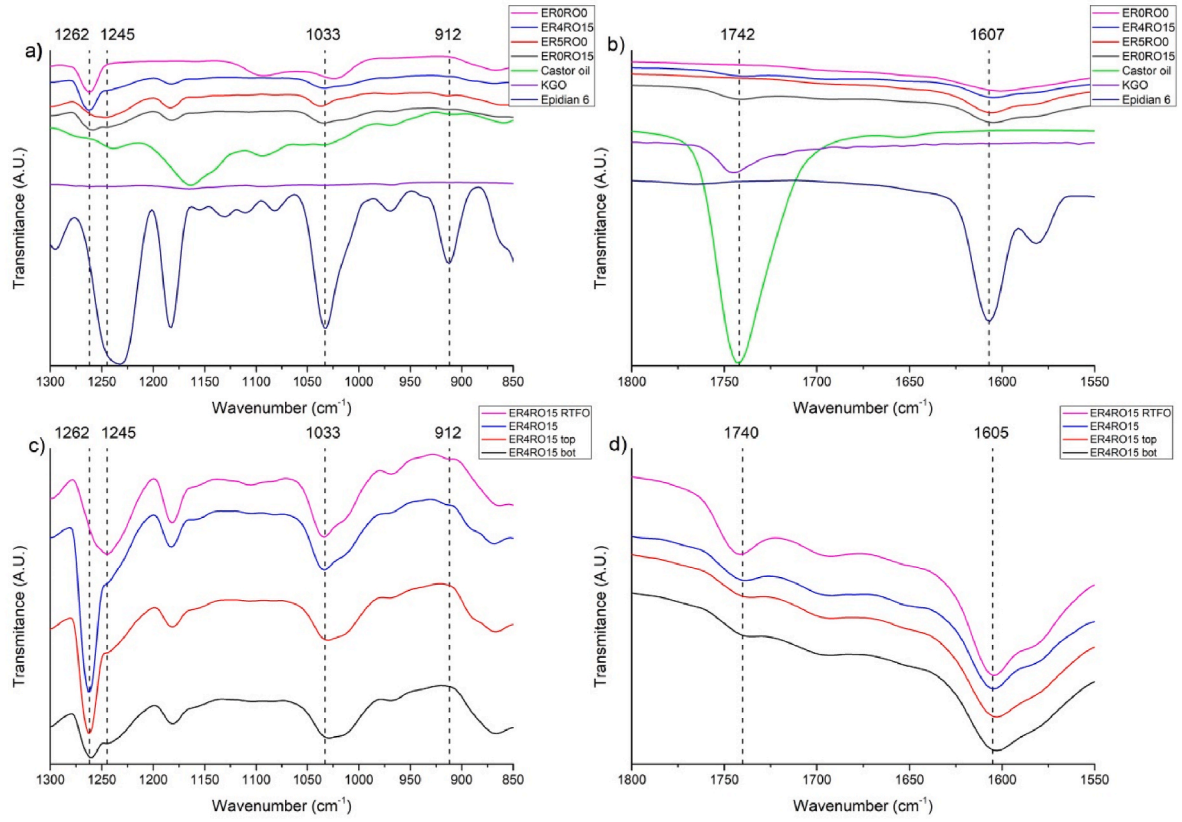

Fig. 9. Transmittance FTIR spectra of modifiers and bitumens after homogenization in two ranges: a) 1300-850 cm^{-1} and b) 1800-1550 cm^{-1}, and of 4ER15RO samples after homogenization, stability test and RTFO in two ranges c) 1300-850 cm^{-1} and d) 1800-1550 cm^{-1}.

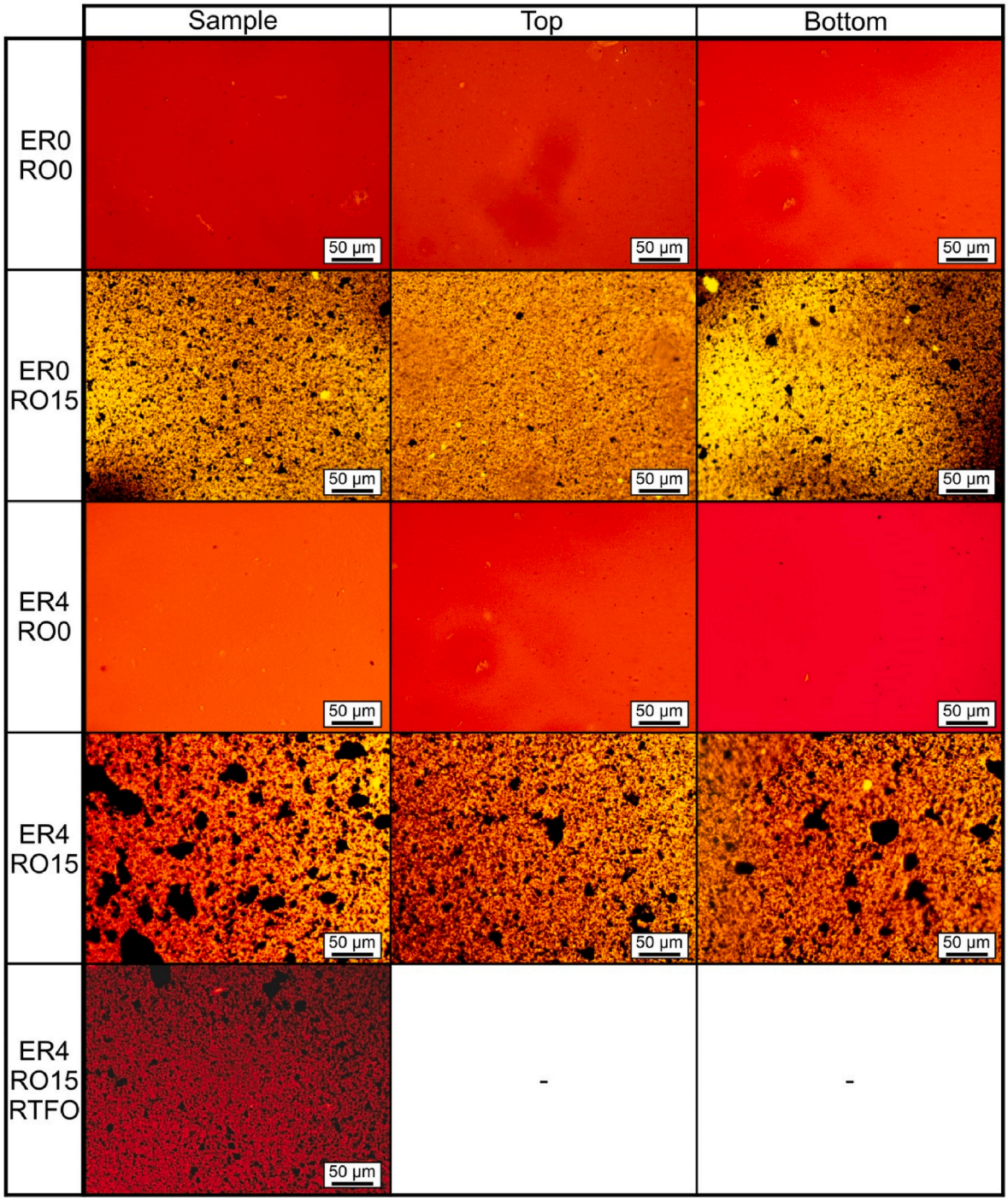

Fig. 10. Micrographs of bitumen samples. Magnification 20x, scale bar 50 μm.

3.4. Optical fluorescence microscopy

In Figs. 10 and 11 micrographs made using conventional transmission and fluorescence mode were presented, respectively. With transmission mode no differences between neat bitumen and epoxy-modified ones are visible. With the addition of RO, black particles appear in the micrographs. No significant differences between samples after homogenization and stability test can be observed for ERxRO0 samples. Only for samples with RO added, it can be spotted that, in the top sample, the visible rubber fraction is smaller compared to the bottom part. Comparing ER4RO15 samples, in the RTFO sample shift to red color can be observed. In fluorescence mode all of the presented samples exhibited fluorescence effect. It is due to aromatic compounds present in neat bitumen. Moreover, it can be spotted that addition of both RO and ER results in increase of bright parts on the micrographs in comparison to ER0RO0. These bright parts are modified bitumen phases rich in conjugated bond systems from ER and RO. It appears that ER gives rise to the development of a new micro-segregated epoxy-rich phase. The dual phase system can be observed, where bitumen phase is continuous and interlocks the epoxy phase. Epoxy resin is well dispersed, and its phase size is small and uniform. RO is also well dispersed and partial swelling of RO can be observed, suggested by partial disappearance of black dots. It is also visible that additional heat treatment affects the number of bright spots – the conjugated bonds from modifiers undergo

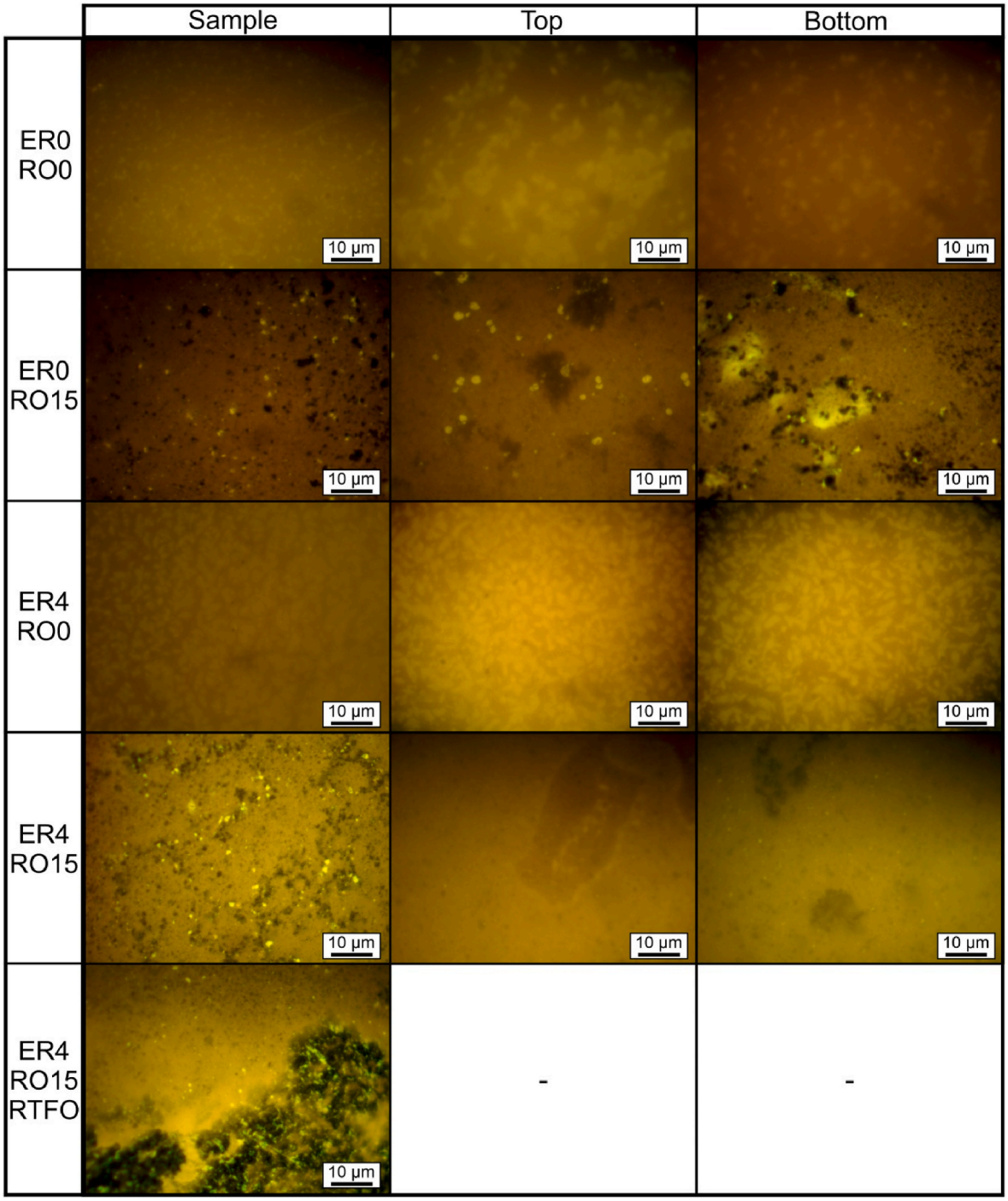

Fig. 11. Fluorescence micrographs of bitumen samples. Magnification 60x, scale bar 10 μm.

reactions with each other and bitumen matrix. In the case of ER4RO15 bitumen, complete disappearance of bright spots can be observed after additional heat treatment. Similar micrographs of epoxy-modified bitumens after homogenization were presented by Gao et al. (2020), although the amount of epoxy-rich phase is much smaller compared to this study. The appearance of bright spots in case of CR-modified bitumen was reported by Yao et al. (2018).

3.5. Contact angle, surface energy, bond energy, and compatibility ratio

In Table 4 the measured contact angles for bitumen samples were shown, as well as calculated surface energies. In all of the studied samples, apart from one sample (0ER15RO TOP), the increase in water contact angle was observed after tube test. This behavior may lead to lower water penetration of asphalt. The addition of RO into bitumen increases the water contact angle, while the addition of ER lowers it. The contact angle of EG and DJM has increased for all modified samples. Calculated dispersive and total surface energy is higher for neat bitumen (ER0RO0), while polar energies are higher for modified samples. In Table 5 results of CoR calculations and changes in % in comparison to neat bitumen were shown. Hefer et al. (2006) proposed this parameter to rank asphalt pavement mixes in terms of the susceptibility for water penetration presented as work of adhesion in dry conditions to the free energy released in wet conditions. The higher this parameter is, the

Table 4
Results of contact angle measurements and surface energy of solid calculations using Van Oss-Good model. Standard errors were below 5%, thus not presented.

Sample	Contact angle [°]			Surface Energy of Solid [mJ/m^2]				
	DJM	EG	Water	Polar	Dispersive	Total	Polar [+]	Polar [-]
ER0RO0	21.60	49.27	84.23	0.2	47.3	47.5	0.01	2.2
ER0RO0 TOP	23.17	63.96	86.2	−3.3	46.8	43.5	0.59	4.5
ER0RO0 BOT	29.60	70.13	92.33	−2.8	44.4	41.6	0.76	2.6
ER0RO15	31.79	73.74	90.67	−4.9	43.5	38.6	1.30	4.7
ER0RO15 TOP	26.50	63.99	82.85	−4.3	45.6	41.3	0.65	7.1
ER0RO15 BOT	29.48	57.44	92.33	−2.7	44.4	41.8	0.02	8.8
ER4RO0	30.46	66.77	81.96	−5.7	44.0	38.3	0.89	9.1
ER4RO0 TOP	28.43	62.22	84.14	−2.9	44.9	42.0	0.37	5.6
ER4RO0 BOT	34.70	61.45	82.80	−2.3	42.2	39.9	0.20	6.5
ER4RO15	30.46	66.77	81.96	−5.7	44.0	38.3	0.89	9.1
ER4RO15 TOP	37.33	71.47	89.65	−3.7	40.9	37.2	0.73	4.8
ER4RO15 BOT	33.16	68.76	84.74	−5.1	42.9	37.8	0.86	7.5
ER4RO15 RTFO	27.70	60.80	93.91	−0.3	45.1	44.8	0.05	0.5

Table 5
Results of compatibility ratio calculations.

Sample	Compatibility ratio									
	Gravel	Change [%]	Granite	Change [%]	Limestone	Change [%]	Basalt	Change [%]	Sandstone	Change [%]
ER0RO0	0.61	–	0.93	–	1.42	–	3.45	–	1.23	–
ER0RO0 TOP	1.02	67%	1.36	46%	1.52	7%	4.64	35%	2.41	96%
ER0RO0 BOT	1.05	72%	1.49	60%	1.42	1%	5.64	64%	2.61	113%
ER0RO15	1.28	111%	1.66	79%	1.50	6%	5.66	64%	3.53	188%
ER0RO15 TOP	1.06	74%	1.31	41%	1.61	14%	3.99	16%	2.47	101%
ER0RO15 BOT	0.83	36%	1.00	8%	1.68	19%	2.91	−16%	1.71	39%
ER4RO0	1.16	91%	1.36	46%	1.66	17%	3.87	12%	2.80	129%
ER4RO0 TOP	0.91	49%	1.18	26%	1.56	10%	3.71	8%	1.99	63%
ER4RO0 BOT	0.80	31%	1.01	8%	1.58	11%	3.03	−12%	1.65	34%
ER4RO15	1.43	135%	1.87	101%	1.49	5%	6.76	96%	4.39	258%
ER4RO15 TOP	1.03	69%	1.33	43%	1.49	5%	4.22	22%	2.44	99%
ER4RO15 BOT	1.13	85%	1.36	46%	1.60	13%	4.01	16%	2.72	121%
ER4RO15 RTFO	0.62	2%	1.05	13%	1.27	−10%	4.51	31%	1.31	7%

better for asphalt, because it indicates high bonding to aggregate and low susceptibility to water. All of the modified bitumen showed higher CoR in comparison to neat bitumen. For gravel, granite, basalt and sandstone the highest CoR were observed for ER4RO15 sample. This is another evidence of reaction of ER and RO in bitumen, due to the synergistic effect of modifiers on CoR. For limestone it is hard to pick the best bitumen. Studied samples after tube test in comparison to samples after homogenization exhibited lowered CoRs for gravel, granite, basalt, and sandstone. In the case of limestone samples with RO showed the opposite effect. The overall highest uplift in CoR was observed in the case of sandstone and sample ER4RO15 – 258% compared to neat bitumen. It is also worth mentioning that the sample preparation method orientates the molecules on the bitumen surface in an open atmosphere. However, in asphalts, the polar moieties are reorienting while mixing with aggregates, which results in higher mobility there, compared to a frozen orientation on glass (Hefer et al., 2006). It is expected that observed uplift in CoR will be even higher in real world asphalt. The CoR is significant for predicting performance of bitumen mixtures in case of moisture damage. The higher the CoR is, the stronger the bond between the bitumen and the aggregates is (Hossain et al., 2015). It is also proposed that CoR>1.5 means “very good” compatibility (Hossain et al., 2015). Increasing contact angle with content of crumb rubber was observed by Habal et al. for both water and EG (Habal and Singh, 2017). Hossain et al. reports uplift in CoR with increasing amount of crumb rubber in PG 64-22 bitumen in comparison to neat bitumen: for 15 wt% of crumb rubber – 1.33, 3.2, 1.6, 4.01 and 1.5 (gravel, granite, limestone, basalt and sandstone respectively). In the case of ER modified bitumen, Cong et al. reports a slight increase in contact angle of water and EG (Cong et al., 2016).

4. Conclusions

Bitumen modification was carried out and discussed herein applying variable amount of rubber-oil mixture (0–20 wt%) and epoxy resin (0–6 wt%). The RO consisted of 90 wt% of rubber dust and 10 wt% of castor oil processed in the mixer at elevated temperature. The modified bitumen was then investigated for the penetration, softening point, and storage stability as well as rheological properties and the estimated compatibility with different aggregates. Overall, the following insights are provided.

- The bitumen specimens modified with RO had a higher storage stability and lower viscosity in comparison with those solely modified with CR. The assigned samples also revealed higher elastic recovery of binder (up to 37.6 ± 3.5%) during MSCR tests.
- Modification of bitumen with ER induced an indiscernible effect on the bitumen properties right after homogenization. However, samples undertaken stability tests showed significantly lower penetration (decreased by ~60%) and an increased softening point (up to ~40%) which could be a signature of creation of polymeric networks in the bitumen matrix.
- Combination of ER and RO allowed obtaining a stable binder with improved rheological and physico-mechanical properties. The resulting binder was signaled by a high UCT, both after stability (77.0°C) and RTFO test (75.5°C) together with high elastic recovery, up to about 48% (ER5RO15 STAB).
- The binder modified with combination of ER and RO was also characterized by the highest CoR, as featured by investigations on surface properties. This sample was predicted to show the best overall compatibility with aggregates, especially gravel and

sandstone, as of the predicted compatibility being almost 260% higher than that of neat bitumen.

The results of this survey suggest that the implementation of the proposed bitumen based binders reinforced with the reclaimed rubber and bio-based oils together with epoxy resins may take the advantage of eliminating the need for petroleum-based modifiers typically used in bitumen industry over an intermediate-to long-term period. This could potentially be a breakthrough outcome to minimize the negative impacts of commercially available bitumen modifiers on the environment. Nevertheless, further studies should focus on optimization of cross-linking time in the course of homogenization process. Additionally, it seems essential to examine how utilizing bio-based catalysts may facilitate the cross-linking reaction applying bio-based ERs based on vegetable oils and plant leaves replacing the commercial ER served in this survey.

CRediT authorship contribution statement

Maciej Sienkiewicz: Conceptualization, Formal analysis, Investigation, Methodology, Project administration, Resources, Supervision, Validation, Writing – original draft, Writing – review & editing. **Przemysław Gnatowski:** Data curation, Formal analysis, Investigation, Software, Visualization, Writing – original draft, Writing – review & editing. **Mateusz Malus:** Investigation, Writing – review & editing. **Anna Grzegórska:** Data curation, Investigation, Methodology. **Hossein Ipakchi:** Software, Visualization, Formal analysis. **Maryam Jouyandeh:** Visualization, Investigation. **Justyna Kucińska-Lipka:** Supervision, Writing – review & editing. **Francisco Javier Navarro:** Investigation, Supervision, Validation, Writing – review & editing. **Mohammad Reza Saeb:** Writing – original draft, Writing – review & editing, Formal analysis.

Declaration of competing interest

The authors declare that they have no known competing financial interests or personal relationships that could have appeared to influence the work reported in this paper.

Data availability

Data will be made available on request.

Acknowledgements

This research did not receive any specific grant from funding agencies in the public, commercial, or not-for-profit sectors.

References

Agudelo, G., Cifuentes, S., Colorado, H.A., 2019. Ground tire rubber and bitumen with wax and its application in a real highway. J. Clean. Prod. 228, 1048–1061. https://doi.org/10.1016/j.jclepro.2019.04.353.

Baensch-Baltruschat, B., Kocher, B., Stock, F., Reifferscheid, G., 2020. Tyre and road wear particles (TRWP) - a review of generation, properties, emissions, human health risk, ecotoxicity, and fate in the environment. Sci. Total Environ. 733, 137823 https://doi.org/10.1016/j.scitotenv.2020.137823.

Bhasin, A., Little, D.N., Vasconcelos, K.L., Masad, E., 2007. Surface free energy to identify moisture sensitivity of materials for asphalt mixes. Transp. Res. Rec. J. Transp. Res. Board 2001, 37–45. https://doi.org/10.3141/2001-05.

Bhasin, A., Masad, E., Little, D., Lytton, R., 2006. Limits on adhesive bond energy for improved resistance of hot-mix asphalt to moisture damage. Transp. Res. Rec. J. Transp. Res. Board 1970, 2–13. https://doi.org/10.1177/0361198106197000101.

Bilema, M., Aman, M.Y., Hassan, N.A., Al-Saffar, Z., Mashaan, N.S., Memon, Z.A., Milad, A., Yusoff, N.I.M., 2021. Effects of waste frying oil and crumb rubber on the characteristics of a reclaimed asphalt pavement binder. Materials 14, 3482. https://doi.org/10.3390/ma14133482.

Borinelli, J.B., Blom, J., Jacobs, G., Hernando, D., Van den Bergh, W., Vuye, C., 2022. Microstructural and rheological analysis of crumb rubber modified bitumen. In: Green and Intelligent Technologies for Sustainable and Smart Asphalt Pavements - Proceedings of the 5th International Symposium on Frontiers of Road and Airport Engineering, IFRAE 2021. CRC Press, London, pp. 599–604. https://doi.org/10.1201/9781003251125-96.

Borinelli, J.B., Blom, J., Portillo-Estrada, M., Kara De Maeijer, P., Van den bergh, W., Vuye, C., 2020. Correction: VOC emission analysis of bitumen using proton-transfer reaction time-of-flight mass spectrometry. Materials 13, 3659. https://doi.org/10.3390/MA13173659.

Bulatović, V.O., Rek, V., Marković, K.J., 2014. Effect of polymer modifiers on the properties of bitumen. J. Elastomers Plast. 46, 448–469. https://doi.org/10.1177/0095244312469964.

Ciech, 2023. Epidian [WWW Document]. URL. https://ciechgroup.com/produkty/pianki-poliuretanowe/zywice/zywice-epoksydowe/, 4.20.23.

Cong, P., Tian, Y., Liu, N., Xu, P., 2016. Investigation of epoxy-resin-modified asphalt binder. J. Appl. Polym. Sci. 133 https://doi.org/10.1002/app.43401 n/a-n/a.

Cuadri, A.A., Delgado-Sánchez, C., Navarro, F.J., Partal, P., 2020. Short-and long-term epoxy modification of bitumen: modification kinetics, rheological properties, and microstructure. Polymers 12, 508. https://doi.org/10.3390/polym12030508.

Çubuk, M., Gürü, M., Çubuk, M.K., 2009. Improvement of bitumen performance with epoxy resin. Fuel 88, 1324–1328. https://doi.org/10.1016/j.fuel.2008.12.024.

Daryaee, D., Ameri, M., Mansourkhaki, A., 2020. Utilizing of waste polymer modified bitumen in combination with rejuvenator in high reclaimed asphalt pavement mixtures. Construct. Build. Mater. 235, 117516 https://doi.org/10.1016/j.conbuildmat.2019.117516.

Dong, F., Yu, X., Liu, S., Wei, J., 2016. Rheological behaviors and microstructure of SBS/CR composite modified hard asphalt. Construct. Build. Mater. 115, 285–293. https://doi.org/10.1016/j.conbuildmat.2016.04.057.

Duan, H., Zhu, C., Li, Y., Zhang, H., Zhang, S., Xiao, F., Amirkhanian, S., 2021. Effect of crumb rubber percentages and bitumen sources on high-temperature rheological properties of less smell crumb rubber modified bitumen. Construct. Build. Mater. 277, 122248 https://doi.org/10.1016/j.conbuildmat.2021.122248.

Eurostat, 2019. Passenger Cars in the EU Statistics Explained. Eurostat Stat. Explain [WWW Document]. https://ec.europa.eu/eurostat/statistics-explained/index.php?title=Passenger_cars_in_the_EU%0Ahttps://ec.europa.eu/eurostat/statisticsexplained/, 4.20.23.

Fathollahi, A., Makoundou, C., Coupe, S.J., Sangiorgi, C., 2022. Leaching of PAHs from rubber modified asphalt pavements. Sci. Total Environ. 826, 153983 https://doi.org/10.1016/j.scitotenv.2022.153983.

Gao, M., Xue, Y., Guan, P., Yuan, F., 2020. Influence mechanism of epoxy resin and curing agent on high-temperature performance of asphalt. Sains Malays. 49, 661–669. https://doi.org/10.17576/jsm-2020-4903-21.

Habal, A., Singh, D., 2017. Moisture damage resistance of GTR-modified asphalt binders containing WMA additives using the surface free energy approach. J. Perform. Constr. Facil. 31, 04017006 https://doi.org/10.1061/(asce)cf.1943-5509.0000995.

Hajikarimi, P., Fakhari Tehrani, F., Moghadas Nejad, F., Absi, J., Rahi, M., Khodaii, A., Petit, C., 2019. Mechanical behavior of polymer-modified bituminous mastics. I: experimental approach. J. Mater. Civ. Eng. 31, 1–10. https://doi.org/10.1061/(asce)mt.1943-5533.0002548.

Hefer, A.W., Bhasin, A., Little, D.N., 2006. Bitumen surface energy characterization using a contact angle approach. J. Mater. Civ. Eng. 18, 759–767. https://doi.org/10.1061/(asce)0899-1561(2006)18:6(759).

Hong, Z., Yan, K., Wang, M., You, L., Ge, D., 2022. Low-density polyethylene/ethylene–vinyl acetate compound modified asphalt: optimal preparation process and high-temperature rheological properties. Construct. Build. Mater. 314, 125688 https://doi.org/10.1016/j.conbuildmat.2021.125688.

Hossain, Z., Bairgi, B., Belshe, M., 2015. Investigation of moisture damage resistance of GTR-modified asphalt binder by static contact angle measurements. Construct. Build. Mater. 95, 45–53. https://doi.org/10.1016/j.conbuildmat.2015.07.032.

Jamal, M., Giustozzi, F., 2020. Low-content crumb rubber modified bitumen for improving Australian local roads condition. J. Clean. Prod. 271, 122484 https://doi.org/10.1016/j.jclepro.2020.122484.

Jamshidi, A., White, G., Kurumisawa, K., 2022. Rheological characteristics of epoxy asphalt binders and engineering properties of epoxy asphalt mixtures–state-of-the-art. Road Mater. Pavement Des. 23, 1957–1980. https://doi.org/10.1080/14680629.2021.1963814.

Järlskog, I., Strömvall, A.M., Magnusson, K., Gustafsson, M., Polukarova, M., Galfi, H., Aronsson, M., Andersson-Sköld, Y., 2020. Occurrence of tire and bitumen wear microplastics on urban streets and in sweepsand and washwater. Sci. Total Environ. 729, 138950 https://doi.org/10.1016/j.scitotenv.2020.138950.

Jeong, K.D., Lee, S.J., Amirkhanian, S.N., Kim, K.W., 2010. Interaction effects of crumb rubber modified asphalt binders. Construct. Build. Mater. 24, 824–831. https://doi.org/10.1016/j.conbuildmat.2009.10.024.

Kaya, D., Topal, A., McNally, T., 2019. Relationship between processing parameters and aging with the rheological behaviour of SBS modified bitumen. Construct. Build. Mater. 221, 345–350. https://doi.org/10.1016/j.conbuildmat.2019.06.081.

Khan, J., Hussain, A., Haq, F., Ahmad, K., Mushtaq, K., 2019. Performance evaluation of modified bitumen with replaced percentage of waste cooking oil & tire rubber with bagasse ash as modifier. Civ. Eng. J. 5, 587. https://doi.org/10.28991/cej-2019-03091270.

Koyun, A.N., Zakel, J., Kayser, S., Stadler, H., Keutsch, F.N., Grothe, H., 2021. High resolution nanoscale chemical analysis of bitumen surface microstructures. Sci. Rep. 11, 13554 https://doi.org/10.1038/s41598-021-92835-3.

Li, H., Zhang, Y., Zhang, M., Cui, C., Hao, G., Zhou, L., 2023. Optimizing parameters for the preparation of low viscosity rubber asphalt incorporating waste engine oil using response surface methodology. Environ. Sci. Pollut. Res. 30, 87433–87448. https://doi.org/10.1007/s11356-023-28383-2.

Li, R., Leng, Z., Partl, M.N., Raab, C., 2021. Characterization and modelling of creep and recovery behaviour of waterborne epoxy resin modified bitumen emulsion. Mater. Struct. Constr. 54, 8. https://doi.org/10.1617/s11527-020-01594-6.
Liu, Q., Han, B., Wang, S., Falchetto, A.C., Wang, D., Yu, B., Zhang, J., 2022. Evaluation and molecular interaction of asphalt modified by rubber particles and used engine oil. J. Clean. Prod. 375, 134222 https://doi.org/10.1016/j.jclepro.2022.134222.
Liu, Q., Liu, J., Yu, B., Zhang, J., Pei, J., Wen, Y., 2023. Preparation and investigation on terminal blend asphalt binders with high content of activated crumb rubber. Int. J. Pavement Eng. 24 https://doi.org/10.1080/10298436.2021.2020271.
Lotos, 2023. Asfalt 70/100 [WWW Document]. URL. https://www.lotosasfalt.pl/1842/p,191,c,1780/produkty_i_cenniki/asfalty_drogowe/asfalt_70/100#tab-2, 4.20.23.
Luo, Z., Zhou, X., Su, Y., Wang, H., Yu, R., Zhou, S., Xu, E.G., Xing, B., 2021. Environmental occurrence, fate, impact, and potential solution of tire microplastics: similarities and differences with tire wear particles. Sci. Total Environ. 795, 148902 https://doi.org/10.1016/j.scitotenv.2021.148902.
Malinowski, S., Wróbel, M., Bandura, L., Woszuk, A., Franus, W., 2022. Use of new green bitumen modifier for asphalt mixtures recycling. Materials 15, 6070. https://doi.org/10.3390/ma15176070.
Motamedi, M., Attar, M.M., Rostami, M., 2017. Performance enhancement of the oxidized bitumen binder using epoxy resin. Prog. Org. Coating 102, 178–185. https://doi.org/10.1016/j.porgcoat.2016.10.011.
Nizamuddin, S., Giustozzi, F., 2022. The role of new compatibilizers in hybrid combinations of waste plastics and waste vehicle tyres crumb rubber-modified bitumen. In: Plastic Waste for Sustainable Asphalt Roads. Elsevier, pp. 165–178. https://doi.org/10.1016/B978-0-323-85789-5.00009-5.
Overlack, 2023. Linseed Oil and Castor Oil [WWW Document]. URL. http://overlack.in.ua/files/Seed_and_castor_oil.pdf, 4.20.23.
Poulikakos, L.D., dos Santos, S., Bueno, M., Kuentzel, S., Hugener, M., Partl, M.N., 2014. Influence of short and long term aging on chemical, microstructural and macro-mechanical properties of recycled asphalt mixtures. Construct. Build. Mater. 51, 414–423. https://doi.org/10.1016/j.conbuildmat.2013.11.004.
Pyshyev, S., Gunka, V., Grytsenko, Y., Bratychak, M., 2016. Polymer modified bitumen: review. Chem. Chem. Technol. 10, 631–636. https://doi.org/10.23939/chcht10.04si.631.
Rødland, E.S., Samanipour, S., Rauert, C., Okoffo, E.D., Reid, M.J., Heier, L.S., Lind, O.C., Thomas, K.V., Meland, S., 2022. A novel method for the quantification of tire and polymer-modified bitumen particles in environmental samples by pyrolysis gas chromatography mass spectroscopy. J. Hazard Mater. 423, 127092 https://doi.org/10.1016/j.jhazmat.2021.127092.
Romera, R., Santamaría, A., Peña, J.J., Muñoz, M.E., Barral, M., García, E., Jañez, V., 2006. Rheological aspects of the rejuvenation of aged bitumen. Rheol. Acta 45, 474–478. https://doi.org/10.1007/s00397-005-0078-7.
Schindelin, J., Arganda-Carreras, I., Frise, E., Kaynig, V., Longair, M., Pietzsch, T., Preibisch, S., Rueden, C., Saalfeld, S., Schmid, B., Tinevez, J.-Y., White, D.J., Hartenstein, V., Eliceiri, K., Tomancak, P., Cardona, A., 2012. Fiji: an open-source platform for biological-image analysis. Nat. Methods 9, 676–682. https://doi.org/10.1038/nmeth.2019.
Shu, X., Huang, B., 2014. Recycling of waste tire rubber in asphalt and portland cement concrete: an overview. Construct. Build. Mater. 67, 217–224. https://doi.org/10.1016/j.conbuildmat.2013.11.027.
Sol-Sánchez, M., Jiménez del Barco Carrión, A., Hidalgo-Arroyo, A., Moreno-Navarro, F., Saiz, L., Rubio-Gámez, M. del C., 2020. Viability of producing sustainable asphalt mixtures with crumb rubber bitumen at reduced temperatures. Construct. Build. Mater. 265, 120154 https://doi.org/10.1016/j.conbuildmat.2020.120154.
Tan, Y., Guo, M., 2013. Study on the phase behavior of asphalt mastic. Construct. Build. Mater. 47, 311–317. https://doi.org/10.1016/j.conbuildmat.2013.05.064.
Tauste-Martínez, R., Moreno-Navarro, F., Sol-Sánchez, M., Rubio-Gámez, M.C., 2021. Multiscale evaluation of the effect of recycled polymers on the long-term performance of bituminous materials. Road Mater. Pavement Des. 22, S99–S116. https://doi.org/10.1080/14680629.2021.1906737.
Tileuberdi, Y., Ongarbaev, Y.K., Mansurov, Z.A., Tuleutaev, B.K., Akkazyn, E.A., 2013. Physical and mechanical characteristics of rubber-bitumen compounds. Chem. Mater. Eng. 1, 105–110. https://doi.org/10.13189/cme.2013.010401.
Van Hal, M., Verbruggen, S.W., Yang, X.Y., Lenaerts, S., Tytgat, T., 2019. Image analysis and in situ FTIR as complementary detection tools for photocatalytic soot oxidation. Chem. Eng. J. 367, 269–277. https://doi.org/10.1016/j.cej.2019.02.154.
Wang, H., You, Z., Mills-Beale, J., Hao, P., 2012. Laboratory evaluation on high temperature viscosity and low temperature stiffness of asphalt binder with high percent scrap tire rubber. Construct. Build. Mater. 26, 583–590. https://doi.org/10.1016/j.conbuildmat.2011.06.061.
Wiśniewska, P., Haponiuk, J.T., Colom, X., Saeb, M.R., 2023a. Green approaches in rubber recycling technologies: present status and future perspective. ACS Sustain. Chem. Eng. 11, 8706–8726. https://doi.org/10.1021/acssuschemeng.3c01314.
Wiśniewska, P., Wójcik, N.A., Ryl, J., Bogdanowicz, R., Vahabi, H., Formela, K., Saeb, M. R., 2023b. Rubber wastes recycling for developing advanced polymer composites: a warm handshake with sustainability. J. Clean. Prod. 427, 139010 https://doi.org/10.1016/j.jclepro.2023.139010.
Xie, H., Li, C., Wang, Q., 2022. A critical review on performance and phase separation of thermosetting epoxy asphalt binders and bond coats. Construct. Build. Mater. 326, 126792 https://doi.org/10.1016/j.conbuildmat.2022.126792.
Xu, N., Wang, Hainian, Wang, Huimin, Kazemi, M., Fini, E., 2023. Research progress on resource utilization of waste cooking oil in asphalt materials: a state-of-the-art review. J. Clean. Prod. 385, 135427 https://doi.org/10.1016/j.jclepro.2022.135427.
Xu, P., Zhu, Z., Wang, Y., Cong, P., Li, D., Hui, J., Ye, M., 2022. Phase structure characterization and compatibilization mechanism of epoxy asphalt modified by thermoplastic elastomer (SBS). Construct. Build. Mater. 320, 126262 https://doi.org/10.1016/j.conbuildmat.2021.126262.
Xue, Y., Ge, D., Lv, S., Duan, D., Deng, Y., 2023. Evaluation of asphalt modified with bio-oil and high rubber content: low temperature and short mixing time production condition. Construct. Build. Mater. 408, 133656 https://doi.org/10.1016/j.conbuildmat.2023.133656.
Yang, H., Dong, R., 2022. Investigating the properties of rejuvenated asphalt with the modified rejuvenator prepared by waste cooking oil and waste tire crumb rubber. Construct. Build. Mater. 315, 125692 https://doi.org/10.1016/j.conbuildmat.2021.125692.
Yao, Z., Zhang, J., Gao, F., Liu, S., Yu, T., 2018. Integrated utilization of recycled crumb rubber and polyethylene for enhancing the performance of modified bitumen. Construct. Build. Mater. 170, 217–224. https://doi.org/10.1016/j.conbuildmat.2018.03.080.
Yin, J., Wang, S., Lv, F., 2013. Improving the short-term aging resistance of asphalt by addition of crumb rubber radiated by microwave and impregnated in epoxidized soybean oil. Construct. Build. Mater. 49, 712–719. https://doi.org/10.1016/j.conbuildmat.2013.08.067.
Zeng, M., Pan, H., Zhao, Y., Tian, W., 2016. Evaluation of asphalt binder containing castor oil-based bioasphalt using conventional tests. Construct. Build. Mater. 126, 537–543. https://doi.org/10.1016/j.conbuildmat.2016.09.072.
Zhang, L., Xing, C., Gao, F., Li, T., shuai, Tan, qiu, Y., 2016. Using DSR and MSCR tests to characterize high temperature performance of different rubber modified asphalt. Construct. Build. Mater. 127, 466–474. https://doi.org/10.1016/j.conbuildmat.2016.10.010.
Zhang, R., Shi, Q., Hu, P., Ji, J., Suo, Z., 2023. Influence of castor oil-based bio-oil on the properties and microstructure of asphalt binder. Construct. Build. Mater. 408, 133564 https://doi.org/10.1016/j.conbuildmat.2023.133564.
Zheng, W., Wang, H., Chen, Y., Ji, J., You, Z., Zhang, Y., 2021. A review on compatibility between crumb rubber and asphalt binder. Construct. Build. Mater. 297, 123820 https://doi.org/10.1016/j.conbuildmat.2021.123820.
Zhu, J., Ahmed, A., Said, S., Dinegdae, Y., Lu, X., 2022. Experimental analysis and predictive modelling of linear viscoelastic response of asphalt mixture under dynamic shear loading. Construct. Build. Mater. 328, 127095 https://doi.org/10.1016/j.conbuildmat.2022.127095.